Interplay between Charge, Orbital, and Magnetic Order in $Pr_{1-x}Ca_xMnO_3$

M. v. Zimmermann,[1] J. P. Hill,[1] Doon Gibbs,[1] M. Blume,[1] D. Casa,[2] B. Keimer,[2,3] Y. Murakami,[4] Y. Tomioka,[5] and Y. Tokura[6]

[1]*Department of Physics, Brookhaven National Laboratory, Upton, New York 11973*
[2]*Department of Physics, Princeton University, Princeton, New Jersey 08544*
[3]*Max-Planck-Institut für Festkörperforschung, 70569, Stuttgart, Germany*
[4]*Photon Factory, Institute of Materials Structure Science, High Energy Accelerator Research Organization, Tsukuba, 305-0801, Japan*
[5]*Joint Research Center for Atom Technology (JRCAT), Tsukuba 305-0046, Japan*
[6]*Department of Applied Physics, University of Tokyo, Tokyo 113-0033, Japan and JRCAT*

(Received 12 May 1999)

We report resonant x-ray scattering studies of charge and orbital order in $Pr_{1-x}Ca_xMnO_3$ with $x = 0.4$ and 0.5. Below the ordering temperature, $T_O = 245$ K, the charge and orbital order intensities follow the same temperature dependence, including an increase at the antiferromagnetic ordering temperature, T_N. High resolution measurements reveal, however, that long range orbital order is never achieved. Rather, an orbital domain state is formed. Above T_O, the charge order fluctuations are more highly correlated than the orbital fluctuations. We conclude that the charge order drives the orbital order at the transition.

PACS numbers: 75.30.Vn, 61.10.Eq, 64.60.Cn

Disentangling the origins of high temperature superconductivity and colossal magnetoresistance in the transition metal oxides remains at the center of current activity in condensed matter physics. An important aspect of these strongly correlated systems is that no single degree of freedom dominates their response. Rather, the ground state properties are thought to reflect a balance among several correlated processes, including orbital and charge order, magnetism, and the lattice degrees of freedom.

The perovskite manganites provide an especially illuminating example of the interplay among these interactions, since in these materials the balance may be altered, for example, by doping. As a result, much work has been done to understand their magnetic ground states and lattice distortions, dating back to the seminal experiments of Wollan and Koehler [1]. Less is known about the roles of charge and orbital order. The classic work of Goodenough [2] has nevertheless served as a guide to their ordered arrangements, as supplemented by measurements of the temperature dependence of the structure and by crystallographic studies. Recently this situation has changed with the detection of charge and orbital order by x-ray resonant scattering techniques [3–10]. Specifically, it has been found that the sensitivity of x-ray scattering to these structures is dramatically enhanced by tuning the incident x-ray energy to the Mn K-absorption edge. Thus, it is now possible to characterize the orbital and charge order in detail, and to study their response to changes of temperature or magnetic field.

In this paper, we report x-ray resonant scattering studies of $Pr_{1-x}Ca_xMnO_3$ with $x = 0.4$ and 0.5. We have detected both charge and orbital order below a common phase transition temperature ($T_O = 245$ K), and confirmed the ground state originally proposed by Goodenough for the isostructural compound $La_{0.5}Ca_{0.5}MnO_3$ [2]. Below the transition, the intensities of the charge and orbital order have the same temperature dependences, suggesting that they are linearly coupled. There is, moreover, an increase in the scattering at the Néel temperature ($T_N = 170$ K), implying a coupling to the magnetic degrees of freedom. Intriguingly, high resolution measurements reveal that long range orbital order is never achieved at these concentrations. Rather, a domain state is formed. At temperatures above T_O, we observe critical charge and orbital scattering. Remarkably, the correlation lengths differ, with the length scale of the charge order exceeding that of the orbital order. From this we conclude that charge order drives the orbital order in these systems. This picture is supported by studies in which the phase transition is driven by an applied magnetic field.

For small x, $Pr_{1-x}Ca_xMnO_3$ has an orbitally ordered ground state at low temperature analogous to that observed in $LaMnO_3$. The electronic configuration of the Mn^{3+} ions is (t_{2g}^3, e_g^1), with the t_{2g} electrons localized. The e_g orbitals are hybridized with the oxygen p orbitals, and participate in a cooperative Jahn-Teller distortion of the MnO_6 octahedra. This leads to $(3x^2 - r^2)$-$(3y^2 - r^2)$–type orbital order of the e_g electrons in the ab plane. For $0.3 \leq x \leq 0.7$, charge order among Mn^{3+} and Mn^{4+} ions is believed to occur in addition to the orbital order. The fraction of Mn ions in the Mn^{4+} state equals the concentration of Ca ions. Thus, by varying the Ca concentration, it is possible to alter the balance between the charge and orbital order. The proposed ground state for $x = 0.4$ is illustrated in Fig. 1b [2,11–13]. In orthorhombic notation, for which the fundamental Bragg peaks occur at $(0, 2k, 0)$ with k integer, the charge order reflections occur at $(0, 2k + 1, 0)$ and the orbital

 0031-9007/99/83(23)/4872(4)$15.00

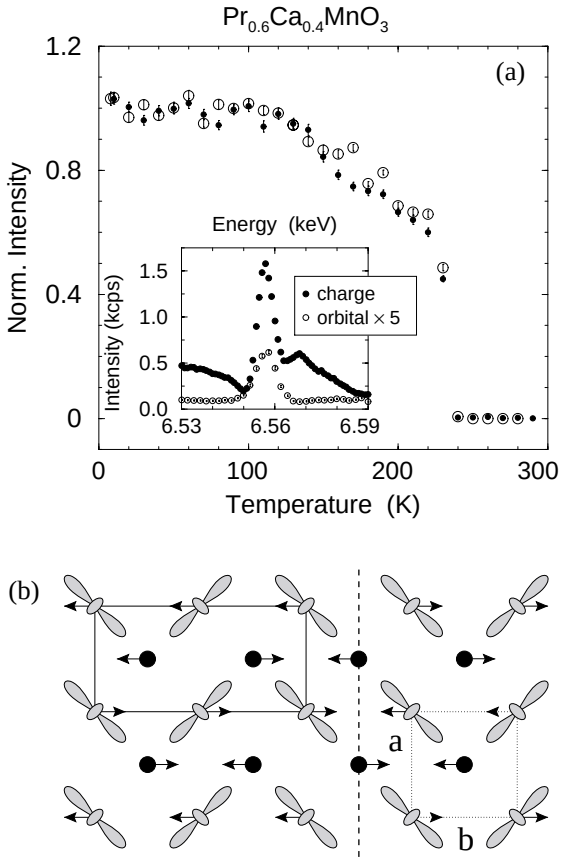

FIG. 1. (a) Orbital and charge order parameters versus temperature for the $x = 0.4$ sample. Open and closed circles: Resonant intensities of the orbital and the charge order measured at the $(0, 1.5, 0)$ and $(0, 3, 0)$ reflections, respectively. Inset: Energy dependence of an orbital $(0, 2.5, 0)$ and charge order $(0, 3, 0)$ peak in the σ-π and σ-σ geometries, respectively. (b) Schematic of charge and orbital order, showing an orbital antiphase domain boundary (dashed line) in the ab plane. Black points represent Mn^{4+} (d^3) and shaded symbols Mn^{3+} (d^4). The arrows indicate the magnetic ordering. The dotted and solid lines show the charge and orbital unit cells, respectively.

order reflections at $(0, k + \frac{1}{2}, 0)$. The magnetic structure is of the modified CE type [11].

The single crystals used were grown by a float zone technique. $(0, 1, 0)$ surfaces were cut and polished giving mosaics of $\sim 0.25°$. Experiments were carried out at the National Synchrotron Light Source on beam line X22C, which utilizes a vertical scattering geometry with an incident energy resolution of ~ 5 eV. Two analyzer configurations were used. The first, a Ge(111) crystal, provided an effective resolution of 7.2×10^{-4} Å^{-1} (HWHM) at the $(0, 2, 0)$ reflection. The second provided polarization analysis with a Cu (220) crystal [14]. The incident polarization was 95% linearly polarized in the horizontal plane (σ). Experiments in a magnetic field were performed on beam line X22B.

The present experiments were carried out using x-ray resonant scattering techniques. As shown in a series of recent papers [3–10], the sensitivity of x-ray scattering to orbital ordering in transition metal oxides is enhanced when the incident x-ray energy is tuned near the K-absorption edge. The resonant scattering may be thought of as Templeton scattering, arising from the anisotropic charge distribution induced by orbital ordering [15,16]. In the dipole approximation, this corresponds to a $1s \rightarrow 4p$ transition at the metal site. The sensitivity to orbital ordering in manganites arises from the splitting of the Mn $4p$ levels as a result of the $3d$ ordering. However, the microscopic origin of this splitting has been controversial [3–10]. Two mechanisms have been proposed. One involves the Coulomb coupling of the Mn $3d$ and Mn $4p$ states, either directly or through the O $2p$ levels [5], while the other involves the perturbation of the O $2p$ and Mn $4p$ wave functions as a result of the Jahn-Teller distortion [7,10]. Insofar as we are aware, the experimental data obtained to date do not distinguish either possibility conclusively, and this remains an open question. Regardless of the microscopic origin, however, the resonant scattering reflects the symmetry of the orbital ordering through the redistribution of the local charge density at the Mn^{3+} sites in both cases. In terms of the Jahn-Teller distortion, specifically, the orientation of the e_g orbitals and the oxygen motion reflect the same order parameter. This is true even if the d orbitals are not directly involved as intermediate states of the resonance. It follows that the peak positions and widths determined in the x-ray experiments measure the orbital periodicity and correlation lengths, respectively. (Supporting evidence for this is given by the consistency of our results and neutron magnetic scattering studies of $La_{1-x}Ca_xMnO_3$ [17] discussed below.) It remains to interpret the x-ray peak intensities on an absolute scale, which we believe will require additional calculations and experiments. The anomalous charge order scattering originates in the small difference in K-absorption energies associated with Mn^{3+} and Mn^{4+} sites as measured at difference reflections.

The inset of Fig. 1 shows the energy dependence of the intensities of the charge and orbital order as the photon energy is tuned through the K-absorption edge. The data were taken at the $(0, 3, 0)$ and $(0, 2.5, 0)$ reflections, respectively, of the $x = 0.4$ sample. Each scan shows an enhancement at 6.555 keV, characteristic of dipole resonant scattering. Maximum count rates of 800 and 3000 s^{-1} were obtained for the orbital and charge order scattering, respectively, with a Ge(111) analyzer. The structure observed in the line shape for the charge order reflects the interference of the resonant and nonresonant contributions, and will be discussed in detail elsewhere [18]. In addition to the resonance, both the charge and orbital order intensities exhibited a $\sin^2(\psi)$ dependence on the azimuthal angle, ψ, at resonance [3,4]. (This angle defines rotations about the scattering vector.) Polarization analysis further revealed that the orbital scattering is predominantly rotated (σ-π), whereas the charge scattering is, to within experimental accuracy, unrotated (σ-σ). These results are consistent with predictions of the resonant cross section for

orbital and charge order [3–5], and confirm the picture of charge and orbital order given for this class of compounds by Goodenough [2] (Fig. 1b).

The temperature dependences of the charge and orbital order obtained at resonance for the $x = 0.4$ sample are shown in Fig. 1. For comparison purposes, the intensities have been scaled together at 10 K. Between 10 and 120 K, both intensities are approximately constant, but decrease by about 25% on passing through the Néel temperature ($T_N = 170$ K). They drop sharply to zero at $T_O = 245$ K. This is coincident with an orthorhombic-to-orthorhombic structural transition, as determined from measurements of the lattice constants [18]. It follows that the temperature dependences of the charge and orbital order are identical, which suggests that the corresponding order parameters are linearly coupled. It seems clear in this regard that the growth of orbital (and charge) order below 245 K enhances the antiferromagnetic correlations, and thereby promotes the magnetic phase transition. This is consistent with the results of inelastic neutron scattering studies of $(Bi, Ca)MnO_3$, in which orbital order was found to quench ferromagnetic fluctuations [19]. Qualitatively similar results have been found for $x = 0.5$ [18].

The behavior of the charge and orbital scattering in the vicinity of the phase transition at T_O is illustrated for the $x = 0.4$ sample in Fig. 2. Longitudinal scans were taken (upon warming) of the $(0, 3, 0)$ reflection in a σ-σ geometry and of the $(0, 2.5, 0)$ reflection in a σ-π geometry. We observe measurable charge order fluctuations (shown on a log scale in Fig. 2a) to much higher temperature above T_O than for the orbital order fluctuations. The corresponding peak widths are considerably narrower for the charge order (Fig. 2b), implying that the correlation lengths of the charge order are longer than those of the orbital order at any given temperature above T_O [20].

The picture these data then present is one in which the phase transition proceeds via local charge order fluctuations which grow as the transition is approached, nucleating long range order at the transition temperature. The orbital fluctuations are induced by these charge fluctuations through the coupling discussed above, and become observable only close to the transition.

The phase transition may also be driven by applying a magnetic field [21]. It is an interesting question as to whether the same phenomenology of the fluctuations applies when the temperature is held fixed. We have carried out studies of the transition at two temperatures, $T = 30$ K (below the magnetic transition) and 200 K (above the magnetic transition), with critical fields of $H_O = 6.9(1)$ T, and $H_O = 10.4$ T, respectively. In agreement with the temperature dependent data, we observed that the two order parameters exhibit identical field dependences below the transition. Above the transition, the charge order fluctuations are markedly stronger than the orbital fluctuations for both temperatures. Thus, it appears that the transition is driven by charge order fluctuations for both temperature and field driven cases.

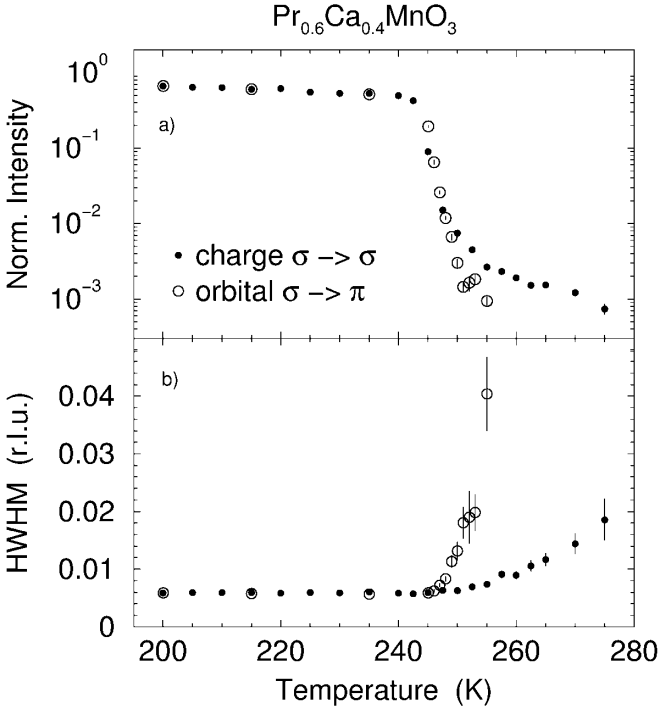

FIG. 2. (a) Temperature dependence of the peak intensities of the$(0, 3, 0)$ charge order peak (closed circles) and the $(0, 2.5, 0)$ orbital order peak (open circles) for the $x = 0.4$ sample. (b) Temperature dependence of the half widths at half maximum (HWHM).

Finally, we performed high q-resolution measurements of the charge and orbital order below T_O to investigate the extent of the order in detail. Remarkably, in the $x = 0.4$ sample, we found an orbital order correlation length of $\xi_{OO} = 320 \pm 10$ Å and a charge order correlation length of $\xi_{CO} \geq 2000$ Å. This difference is even more apparent in the $x = 0.5$ sample, as shown in Fig. 3. Here longitudinal scans through the $(0, 2, 0)$, $(0, 1, 0)$, and $(0, 2.5, 0)$ reflections are superimposed for comparison. The width of the $(0, 2, 0)$ scan approximates the effective resolution. The $(0, 1, 0)$ charge order reflection shows only a slight broadening [$9.1(1) \times 10^{-4}$ Å^{-1}], corresponding to a correlation length of $\xi_{CO} \geq 2000$ Å [22]. The orbital order, however, is substantially broadened, with a correlation length of $\xi_{OO} = 160 \pm 10$ Å [23]. It follows that the orbitals do not exhibit long range order, but instead form a domain state with randomly distributed antiphase domain walls (see Fig. 1b). In contrast, the charge order is much more highly correlated.

A possible explanation for the difference in orbital domain sizes observed in the two samples follows from the fact that the $x = 0.5$ sample is closer to tetragonal than the $x = 0.4$ sample: $\delta(x = 0.5) = \frac{2(a-b)}{(a+b)} = 1.48 \times 10^{-3}$ compared to $\delta(x = 0.4) = 4.23 \times 10^{-3}$ at room temperature [11]. In the more tetragonal sample, the a and b domains are nearly degenerate and the energetic cost of an orbital domain wall is correspondingly reduced [24].

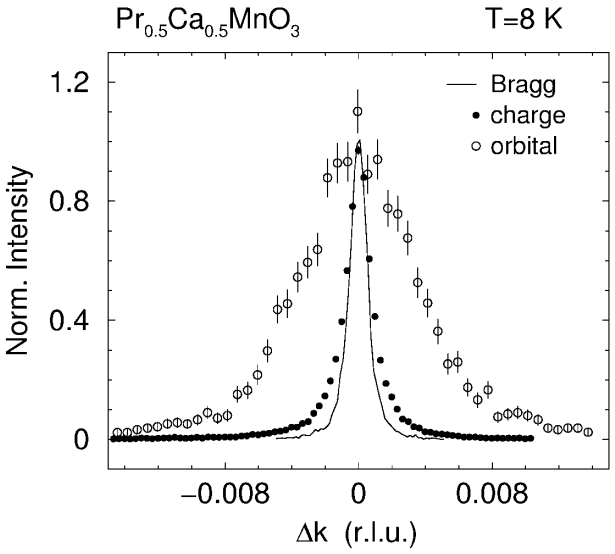

FIG. 3. Longitudinal scans of the $(0, 2, 0)$ Bragg reflection, the $(0, 1, 0)$ charge order peak, and the $(0, 2.5, 0)$ orbital order peak. The orbital order peak is significantly broadened.

The presence of an orbital domain state is consistent with powder neutron diffraction studies of $La_{0.5}Ca_{0.5}MnO_3$, which also exhibits the CE magnetic structure with orbital and charge order [17]. Here, magnetic correlation lengths of $\xi_{3+} = 200{-}400$ Å and $\xi_{4+} \geq 2000$ Å were found for the respective sublattices, and antiphase domain walls were postulated to explain the disorder. It seems likely that these domain walls are the orbital domains observed in the present experiment, which lead to magnetic disorder through the coupling mentioned above. The presence of such orbital domain boundaries breaks the magnetic coherence of the $3+$ sublattice only, as long as charge order is preserved (Fig. 1b). These results taken together suggest that orbital domain states may be common to these systems—at least in this range of doping.

In summary, we have used resonant x-ray scattering techniques to study charge and orbital order in doped manganites, $Pr_{1-x}Ca_xMnO_3$, with $x = 0.4$ and 0.5. We have found that the transition into a charge and orbitally ordered state proceeds via charge order fluctuations, which grow as the transition is approached from above, until at an abrupt, first-order-like transition long range charge order is nucleated. At the same time, less well correlated orbital fluctuations are observed. While the correlation length of the orbital order grows as the transition is approached, long range order is not achieved, and below the charge order transition an orbital domain state is observed. The orbital correlation length appears to be concentration dependent, with a more highly correlated orbital state being observed in the $x = 0.4$ sample. Phenomenologically similar behavior is observed when the phase transition is driven by a magnetic field. Below the transition, the charge and orbital order parameters exhibit identical temperature dependences, indicative of an apparently linear coupling between these degrees of freedom. At the Néel temperature a jump in their intensities is observed demonstrating the importance of the magnetic coupling in these systems.

We acknowledge useful conversations with S. Ishihara, A. J. Millis, and G.A. Sawatzky. The work at Brookhaven was supported by the U.S. Department of Energy, Division of Materials Science, under Contract No. DE-AC02-98CH10886 and at Princeton University by the N.S.F., under Grant No. DMR-9701991. Support from the Ministry of Education, Science and Culture, Japan, by the New Energy and Industrial Technology Development Organization (NEDO), and by the Core Research for Evolutional Science and Technology (CREST) is also acknowledged.

[1] E. O. Wollan and W. C. Koehler, Phys. Rev. **100**, 545 (1955).
[2] J. B. Goodenough, Phys. Rev. **100**, 555 (1955).
[3] Y. Murakami *et al.*, Phys. Rev. Lett. **80**, 1932 (1998).
[4] Y. Murakami *et al.*, Phys. Rev. Lett. **81**, 582 (1998).
[5] S. Ishihara and S. Maekawa, Phys. Rev. Lett. **80**, 3799 (1998).
[6] M. Fabrizio, M. Altarelli, and M. Benfatto, Phys. Rev. Lett. **80**, 3400 (1998); **81**, 4030 (1998).
[7] I. S. Elfimov, V. I. Anisimov, and G. A. Sawatzky, Phys. Rev. Lett. **82**, 4264 (1999).
[8] Y. Endoh *et al.*, Phys. Rev. Lett. **82**, 4328 (1999).
[9] L. Paolasini *et al.*, Phys. Rev. Lett. **82**, 4719 (1999).
[10] M. Benfatto, Y. Joly, and C. R. Natoli, Phys. Rev. Lett. **83**, 636 (1999).
[11] Z. Jirák *et al.*, Magn. Magn. Mater. **53**, 153 (1985).
[12] Y. Okimoto *et al.*, Phys. Rev. B **57**, R9377 (1998).
[13] The CE-type charge order structure is stable for $0.4 < x < 0.7$ in $Pr_{1-x}Ca_xMnO_3$. For $x < 0.5$, the excess electrons are believed to reside in partially occupied $3z^2 - r^2$ orbitals [11].
[14] D. Gibbs *et al.*, Rev. Sci. Instrum. **60**, 1655 (1988).
[15] See, e.g., M. Blume, in *Resonant Anomalous X-ray Scattering*, edited by G. Materlik, C. J. Sparks, and K. Fischer (North-Holland, Amsterdam, 1991), p. 495; A. Kirfel, in *Resonant Anomalous X-ray Scattering*, p. 231.
[16] K. D. Finkelstein, Q. Shen, and S. Shastri, Phys. Rev. Lett. **69**, 1612 (1992).
[17] P. G. Radaelli *et al.*, Phys. Rev. B **55**, 3015 (1997).
[18] M. v. Zimmermann *et al.* (to be published).
[19] Wei Bao *et al.*, Phys. Rev. Lett. **78**, 543 (1997).
[20] The correlation length of the charge order must be at least as long as that of the orbital order, since the unit cell of the orbital order is defined on the charge order lattice.
[21] Y. Tomioka *et al.*, Phys. Rev. B **53**, R1689 (1996).
[22] As estimated by performing a 1D deconvolution of the resolution and using $\xi = \frac{b}{2\pi\Delta k}$, were Δk is the fitted HWHM.
[23] Note the q dependence of the resolution function is much too small to explain the observed broadening.
[24] A. J. Millis (private communication).